

Deep Learning-Based Spectral Extraction for Improving the Performance of Surface-Enhanced Raman Spectroscopy Analysis on Multiplexed Identification and Quantitation

Jie Zhang,[†] Pei-Lin Xin,[†] Xiao-Yuan Wang, Hua-Ying Chen,* and Da-Wei Li*



Cite This: *J. Phys. Chem. A* 2022, 126, 2278–2285



Read Online

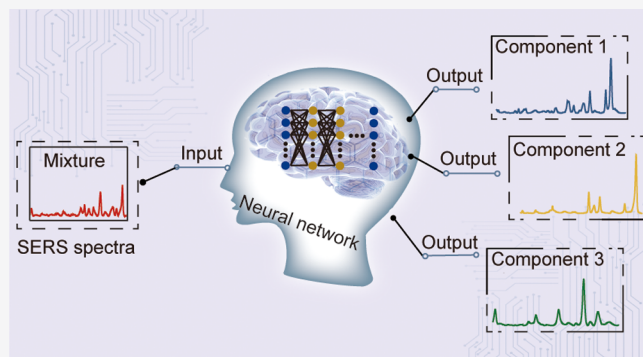
ACCESS |

Metrics & More

Article Recommendations

Supporting Information

ABSTRACT: Surface-enhanced Raman spectroscopy (SERS) has been recognized as a promising analytical technique for its capability of providing molecular fingerprint information and avoiding interference of water. Nevertheless, direct SERS detection of complicated samples without pretreatment to achieve the high-efficiency identification and quantitation in a multiplexed way is still a challenge. In this study, a novel spectral extraction neural network (SENN) model was proposed for synchronous SERS detection of each component in mixed solutions using a demonstration sample containing diquat dibromide (DDM), methyl viologen dichloride (MVD), and tetramethylthiuram disulfide (TMTD). A SERS spectra dataset including 3600 spectra of DDM, MVD, TMTD, and their mixtures was first constructed to train the SENN model. After the training step, the cosine similarity of the SENN model can achieve 0.999, 0.997, and 0.994 for DDM, MVD, and TMTD, respectively, which means that the spectra extracted from the mixture are highly consistent with those collected by the SERS experiment of the corresponding pure samples. Furthermore, a convolutional neural network model for quantitative analysis is combined with the SENN, which can simultaneously and rapidly realize the qualitative and quantitative SERS analysis of mixture solutions with lower than 8.8% relative standard deviation. The result demonstrates that the proposed strategy has great potential in improving SERS analysis in environmental monitoring, food safety, and so on.



INTRODUCTION

Surface-enhanced Raman spectroscopy (SERS) has attracted considerable attention because it is highly sensitive via magnifying the vibrational fingerprint information of analytes with plasmonic structures,^{1–4} such as roughened surfaces of gold and silver.^{5,6} Meanwhile, valuable information can be recorded almost without interference from water when aqueous samples are directly detected.⁷ Hence, SERS is proposed to implement rapid and sensitive qualitative/quantitative analysis and detection in various fields, such as biomolecular and chemical sensing, food safety, and drug monitoring.^{8–13} However, the analysis of complicated SERS spectra obtained from the mixed solutions without pretreatment is still a challenge.¹⁴ Therefore, a separative method¹⁵ or high-performance substrates^{16,17} are developed for mixture analysis; nevertheless, this usually requires tedious processes. In addition, the SERS spectra are still difficult to be artificially analyzed and identified due to the complicity and subtle changes of spectra.¹⁸ In recent decades, several chemometrics methods have emerged for mixtures analysis, such as interactive self-modeling mixture analysis (SIMPLISMA)¹⁹ and iterative target transformation factor analysis (ITTFA).²⁰

However, these methods cannot effectively work because of peaks overlapped for many materials.²¹

Machine learning (ML) has revealed many advantages in various fields.^{22,23} Especially, deep learning (DL) which is a branch of ML is widely used in face identification, and recently, it is emerging as an important analytical method in chemical fields such as substance classification,^{24–26} prediction of concentration,^{27,28} precise cancer detection,²⁹ and virtual molecular projections.³⁰ In recent years, many helpful tools, such as PyTorch and Tensorflow, have been developed by various corporations to conveniently construct a deep learning model. Hence, the neural network (NN) model can be easily and rapidly established by these tools to accomplish the tasks mentioned above, and the compute details of the NN and work pattern would not be excessively concerned. Although component identification of mixtures has been implemented

Received: December 18, 2021

Revised: February 25, 2022

Published: April 5, 2022



Scheme 1. Schematic Illustration of SENN Model Construction for Extracting Pure Spectra of Each Component from Mixture Spectra

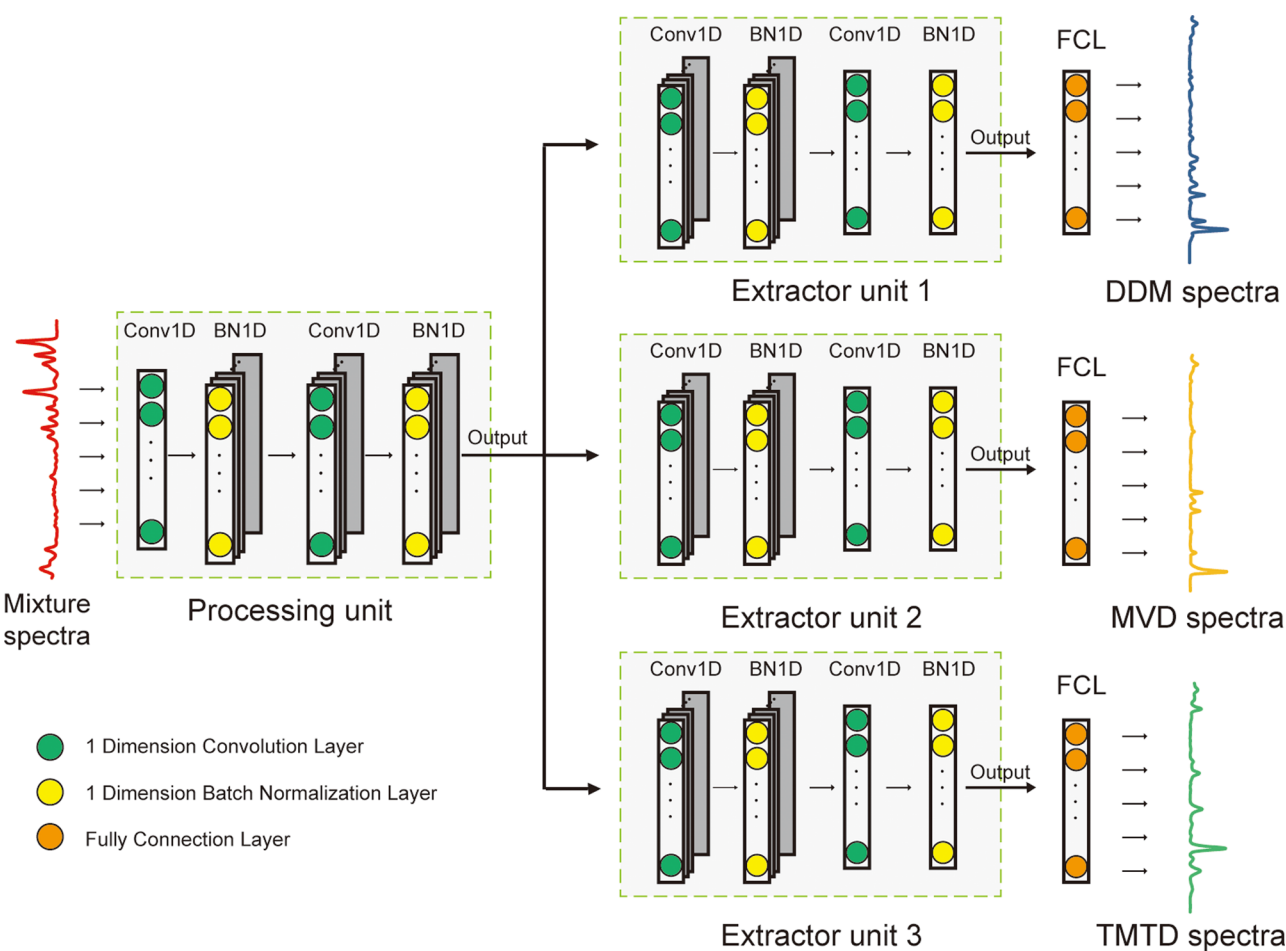
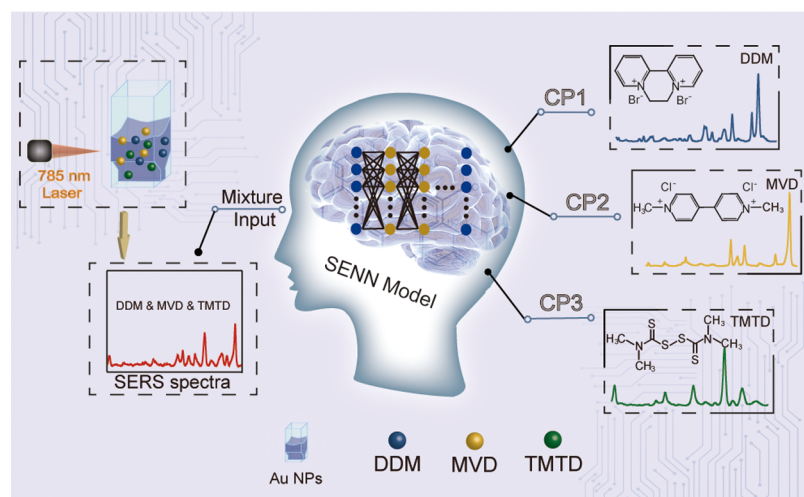


Figure 1. Architecture of SENN. It contains one processing unit and three extractor units. The processing unit and extractor unit 1 include two one-dimension convolutional layers and two one-dimension batch normalization layers. Extractor units also include a linear layer used to restore pure spectra.

by a deep NN called DeepCID,¹⁴ it was still based on the classification strategy. Owing to the strong learning ability of DL, it has potential in extracting pure spectra from mixtures and precisely predicting the concentration of each component in the mixtures. However, to the best of our knowledge, SERS

spectral extraction from the mixtures using the NN has not been proposed yet.

In this work, a DL model called the spectral extraction NN (SENN) was developed based on the NN for extracting pure spectra of each component from mixture spectra (**Scheme 1**). As a proof of concept, the SERS spectra dataset was first

constructed by collecting the SERS spectra of a mixture system containing diquat dibromide (DDM), methyl viologen dichloride (MVD), and tetramethylthiuram disulfide (TMTD), which are widely used in agricultural production and hard to be directly distinguished from each other in their coexisting samples by SERS without pretreatment.^{31–33} Benefiting from functional modular design of the SENN model, the pure spectra extracted from mixture spectra agreed well with the corresponding experiment spectra. The cosine similarity for DDM, MVD, and TMTD was 0.999, 0.997, and 0.994, respectively. The SENN was then combined with a convolutional NN (CNN) which could implement simultaneously quantitative analysis for mixture samples. As a result, concentrations of each component were precisely predicted, showing that the SENN has immense potential in improving the SERS analysis efficiency of the mixtures.

METHODS

Acquisition of SERS. Solutions (1 mM) of DDM, MVD, and TMTD were prepared by using deionized water and dimethyl sulfoxide (DMSO). Subsequently, in order to confirm the appropriate concentration of measurement for them, DDM and MVD solution was diluted into different concentrations from 0.01 to 100 μM , and TMTD solution was diluted into varying concentrations from 0.05 to 100 μM with gold nanoparticles (Au NPs, the synthetic method and characterizations are respectively shown in [Text S1](#) and [Figure S1](#), and condition optimization of SERS detection is shown in [Text S2](#)).

Afterward, SERS spectra were recorded via a portable Raman spectrometer using an excitation wavelength of 785 nm, an integration time of 10 s, and a laser power of 45 mW. To simplify the research work, the concentrations of 0.01, 0.10, and 1.00 μM for DDM and MVD and 0.05, 0.50, and 1.00 μM for TMTD were chosen to collect pure spectra (nine cases). Additionally, the ternary mixed solutions were prepared by their arbitrary combination to acquire mixed spectra (27 cases). For each case of the pure and mixed solutions, 100 spectra were then collected to build the SERS dataset for the SENN model (3600 spectra).

Data Preprocessing and Organization. The SERS spectra dataset needs to be preprocessed before constructing the model by several procedures: (1) baseline correction, (2) clipping, (3) smoothing, and (4) scaling. A baseline correction method, called asymmetric least squares, was used to prevent the impact of baseline drift. Subsequently, the Raman shift of those spectra was clipped from 63–3350 to 400–1750 cm^{-1} to cut all of the useless parts of SERS spectra that do not include any peaks at a high shift or any invalid information at a low shift. Then, the SERS spectra were smoothed by the Savitzky–Golay method using the Scikit-Learn toolbox and a window with a size of 11 and polynomial order 3 as necessary parameters. Finally, the Min–Max scaling method was utilized to scale intensity with a minimum value of 0 and a maximum value of 1. For each ternary mixed case, the pure spectra were used as the labels to compute the similarity to evaluate extractive results at the training and testing step after preprocessing. For example, pure spectra of 0.01 μM DDM, 0.01 μM MVD, and 0.05 μM TMTD were used as labels of their mixture spectra (0.01:0.01:0.05). The final dataset was organized by this way.

Architecture of SENN. As shown in [Figure 1](#), the SENN model can be split into one processing unit (PU) and three

extractor units (EUs). The PU is used to further process the spectra and get the features of input which is spectra of mixtures with one channel. This unit consists of two one-dimension convolutional (Conv1D) layers which are typically used to extract features and two one-dimension batch normalization (BN1D) layers that improve stability of data. The first and second Conv1D are performed by using a sliding window with a size of 3, and their output channels are respectively set as 6 and 12. The BN1Ds are only setting the value of the channel according to the previous Conv1D. Then, output of each BN1D is passed to an activation function ReLU to implement nonlinearity transformation for features.

To extract pure spectra from experimental spectra of mixtures, final output with twelve channels of the PU is directly sent to EUs. EU1 contains two Conv1Ds, two BN1Ds, and a linear layer. Compared with the Conv1D of the PU, the output channels of those two Conv1Ds are six and one, respectively. Subsequently, output of the last BN1D is passed to a fully connected layer with an activation function sigmoid to restore pure spectra. EU2 and EU3 have the same construct with EU1. Size of all layers in the SENN is unaltered and is same as length of original spectra so that this model can furthest retain the information of whole spectra.

Extractive Procedure Formulizing. The preprocessing unit is used to learn about the distribution of features. The convolutional function which can be described by using [eq 1](#) was performed on the spectral vector

$$z_n = \sum_{k=0}^{N-1} x_k g_{n-k} \quad (1)$$

where z is the convolutional result for input of the experimental spectral vector, and $x = [x_1, x_2, \dots, x_{\text{dim}}]^T$, which contains intensities used to build the model. The g is a filter function. The k denotes the k th value of the convolution kernel for the convolutional process.

Batch normalization operation (BNO) is then executed on each batch to prevent gradient diffusion problem. BNO is executed by using the following expression³⁵

$$\hat{z} = \frac{z - \mu_B}{\sqrt{\sigma_B^2 + \epsilon}} \quad (2)$$

where

$$\mu_B = \frac{1}{m} \sum_{i=1}^m z_i$$

$$\sigma_B^2 = \frac{1}{m} \sum_{i=1}^m (z_i - \mu)^2$$

and the m is the number of samples in each batch; additionally, the ϵ is added to avoid the divide 0 error. Then, the final processing result can be obtained by using

$$\tilde{z} = \gamma \hat{z} + \beta \quad (3)$$

where γ and β are trainable hyper-parameters.

The final \tilde{z} obtained from the preprocessing unit could be regarded as feature space, which is used to restore pure spectra.

Once the final \tilde{z} has been obtained upon, it can be passed into the extractor unit. The convolutional operation and BNO are same as [eqs 1](#) and [2](#), respectively. Additionally, the extractive spectra could be described by using the following equation

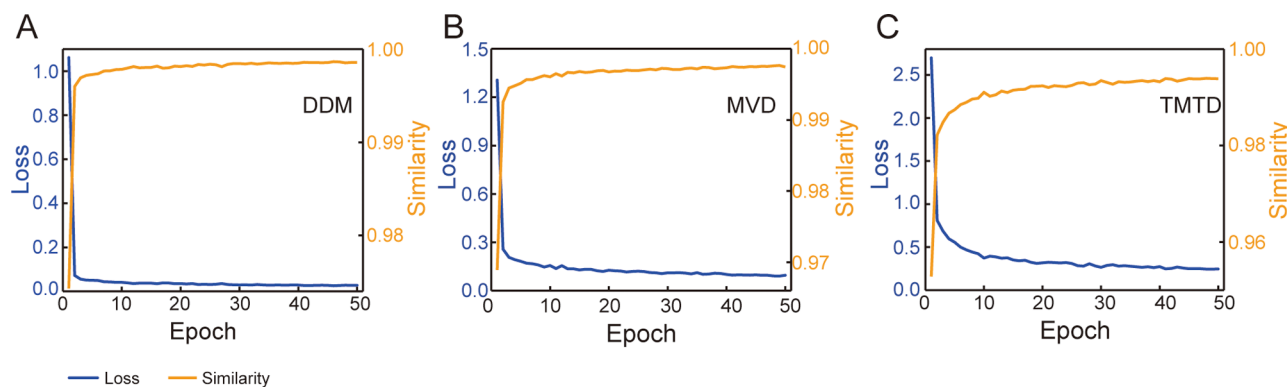


Figure 2. Training results for DDM (A), MVD, (B) and TMTD (C). Blue line: MSE loss over gradient descent steps of the model and yellow line: cosine similarity over gradient descent steps of the model.

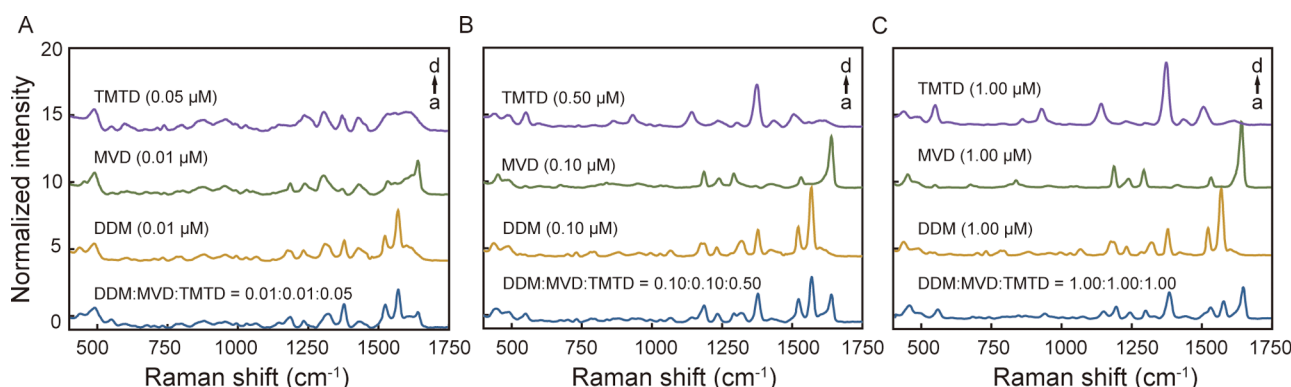


Figure 3. Extractive results for mixture spectra involving varying concentrations of DDM, MVD, and TMTD using the SENN. For the graph of (A–C), a: experimental mixture spectra and b, c, and d: extracted pure spectra of DDM, MVD, and TMTD, respectively.

$$s = f(W\bar{z} + b) \quad (4)$$

where s is the extractive spectrum, and f is the sigmoid function which is used to transfer the output corresponding values in the range of 0 to 1²⁶

$$f(x) = \frac{1}{1 + e^{-x}}$$

Although pure spectra could be recovered by using eq 4, the evaluation of extractive quality is still a problem. In general, distance between two vectors can be used to represent their similarity. Here, cosine similarity is used to evaluate the similarity between extractive pure spectra and corresponding experimental spectra which could be expressed by using eq 5

$$\text{similarity} = \frac{s \cdot x}{\max(\|s\|_2 \cdot \|x\|_2, \epsilon)} \quad (5)$$

RESULTS AND DISCUSSION

Performance of SENN. To train the model, the SENN model dataset containing 3600 spectra was first preprocessed and then randomly split into 2 segments: training set (90%) and testing set (10%). The former one was used to train the SENN model to learn the hyper-parameters for each layer, and the latter one was used to test the extraction ability of this model. Moreover, the mean square error (MSE) loss function and adaptive moment estimation (Adam) optimizer were selected to be the target function and adjust all hyper-parameters, respectively. The SENN model differs from the classification model, so the accuracy cannot be used to evaluate

results of the model because the output of the SENN is the spectrum rather than the category. Hence, in this work, cosine similarity was chosen to describe the quality of extraction and the training process for extractive spectra.

For DDM, the MSE dramatically decreased from 1.062 to 0.072 after the first epoch renovating of hyper-parameters and then slowly decreased to an almost constant value (0.027) (shown in Figure 2A). Meanwhile, the similarity between predicted spectra and experimental spectra increased from 0.974 to 0.999. As for MVD and TMTD, similar trends were observed as shown in Figure 2B,C, and the MSE (0.096 and 0.245 for MVD and TMTD, respectively) and cosine similarity (0.997 and 0.994 for MVD and TMTD, respectively) also respectively reached a stable value after 50 epochs. Therefore, the SENN model was saved as a document with extension of ".pt" after 50 iterations and used to extract pure spectra from mixture spectra.

Once the SENN model had been trained and saved upon, it could be easily used by reloading from the disk. The SENN model was first tested at the test set, and its results showed that the MSE was 0.009 (DDM), 0.037 (MVD), and 0.072 (TMTD), and the cosine similarity was 0.991 (DDM), 0.990 (MVD), and 0.986 (TMTD). Subsequently, three kinds of mixture spectra belonging to different concentrations were selected to visualize, and the results are shown in Figure 3. For mixture solution of DDM (0.01 μM), MVD (0.01 μM), and TMTD (0.05 μM) in Figure 3A, the mixture spectrum (a) was recorded by the experimental process, and pure spectra of DDM (b), MVD (c), and TMTD (d) were then extracted from the mixture spectrum by the SENN model, and their pure

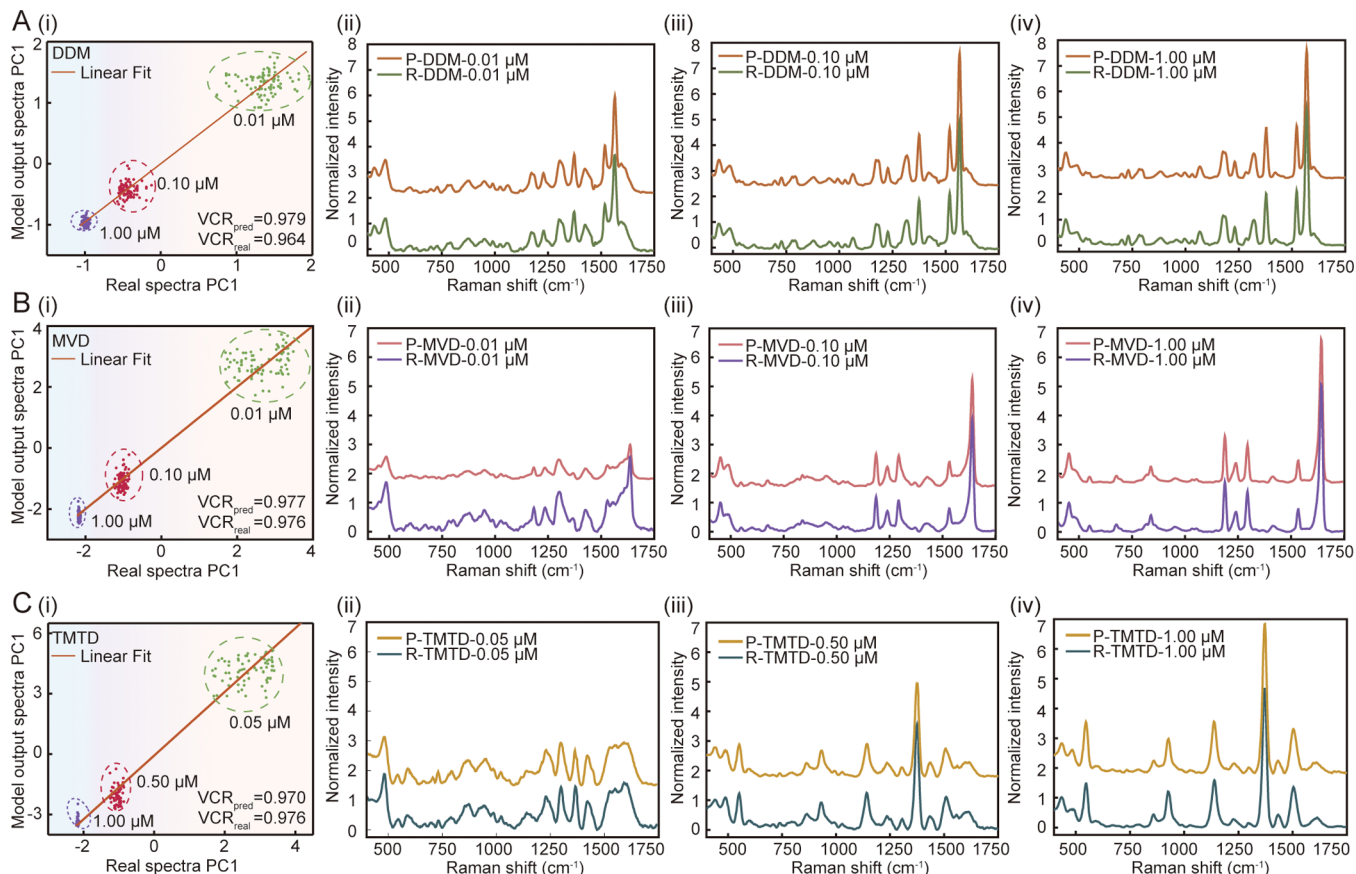


Figure 4. Quality evaluation of pure spectra using PCA. The PCA results for DDM [4A(i)], MVD [4B(i)], and TMTD [4C(i)]. PC1 of real spectra extracted from experiments as the X-axis and PC1 of pure spectra extracted from mixture spectra as the Y-axis. The bottom-right corner shows VCR of both extracted and experimental spectra. (ii–iv) of (A–C), pure spectra extracted from different mixture spectra compared with corresponding experiment spectra for MVD and TBZ in each concentration. Note: taking A(ii) as an example, P-DDM-0.01 μM means that DDM (0.01 μM) extracted (predicted) from the SENN model, R-DDM-0.01 μM , means that DDM (0.01 μM) was acquired from the experiment.

spectra were in complete agreement with the spectra acquired from experiments (Figure S2). Moreover, the collected pure spectra of DDM (or MVD and TMTD) with three concentrations were stable (Figure S3). Likewise, pure spectra could be extracted from mixture spectra with different concentrations displayed in Figures 3B,C. Finally, the extractive results of other 24 cases are listed in Figures S4 and S5.

In addition, interactive SIMPLISMA, which is based on pure variables, had been proposed by Windig in 1991.¹⁹ In Windig's research, they assume that pure variables are present. However, inferior resolution results would be obtained by SIMPLISMA because poor pure variables were selected.²¹ To more intuitively show the advantage of the SENN, Windig's method implemented by ourselves using Python was performed only on the same mixture spectra set of the same test set. The resolution components were nearly same as those of the mixture spectra (Figure S6A–C), which suggested that there is no extractive effect for datasets which only include mixture spectra by SIMPLISMA. These results further indicate that the SENN model can effectively extract the spectra of pure components from the mixtures.

Principal Component Analysis for the Quality of Spectral Extraction. For the purpose of further evaluating the quality of spectra extracted by the SENN model, the analysis method was considered. The SRES spectra cannot be visualized directly because they are high-dimension vectors.

Hence, a decomposing method is needed for visualization of high-dimension data. Principal component analysis (PCA) is usually used to reduce the dimension of high-dimensional data, minimize the information loss of data, and improve the interpretability.³⁶ Here, PCA was chosen to reduce all information of a whole SERS spectra into one variable extracted and acquired from experiments of pure spectra.

PCA was performed on the test set, and only the first principal components (PC1) remain. For DDM, the variance contribution rate (VCR), which can describe the information ratio of a principal component on whole spectra, was 0.964 and 0.979 for experimental spectra and extractive spectra, respectively (Figure 4A). The results indicate that either model output spectra PC1s or real spectra PC1s can represent MVD spectra well. On the other hand, PC1s of pure spectra extracted by the SENN model had a good linear relationship with corresponding PC1s of experimental spectra for concentrations of 0.01, 0.10, and 1.00 μM (Figure 4A). Furthermore, the PC1 points, which are composed of real spectra PC1s and extractive spectra PC1s respectively regarded as x and y , concentrated the nearby counter diagonal of the square area, which indicates that extractive pure spectra have unexceptionable quality compared with experimental pure spectra using the SENN. As shown in Figure 4A(ii)–(iv), 0.01, 0.10, and 1.00 μM DDM spectra, which were respectively extracted from different mixture solutions by the SENN model, were compared with corresponding spectra recorded from

experiments. The results suggest that the pure SERS spectra obtained from the SENN and experiments are also highly consistent.

As for MVD (Figure 4B(i)), the results were similar to those of DDM. The VCR is 0.976 and 0.977 for experimental spectra and extractive spectra, respectively. For TMTD, although PC1 points were more discrete than those of DDM and MVD [shown in Figure 4C(i)], they still distributed nearby the counter diagonal, and the VCR is 0.976 and 0.970 for experimental spectra and extractive spectra, respectively. Additionally, the extractive spectra were also matched well with their experimental spectra as shown in Figure 4B,C(ii)–(iv). These results implied that the SENN model has strong ability to extract pure spectra from the mixture spectra from a qualitative perspective.

SERS Quantitative Analysis Using CNN for Extractive Spectra. In fact, according to Figure 4A(i), B(i), C(i), DDM PC1 points, MVD PC1 points, and TMTD PC1 points could be separated into three parts: top-right one, middle one, and bottom-left one. This indicates that concentration information of DDM, MVD, and TMTD in mixture solutions was included in extractive spectra.

Hence, to further verify the concentration information of extractive spectra and show application of the SENN in quantitative analysis, a CNN model (shown in Figure S7) was used to be a quantitative analysis method for DDM and MVD as a proof of concept (the quantification analysis method is shown in Text S3). To train this model, a new dataset that has 1000 pure spectra of DDM and MVD with different concentrations is constructed using experimental spectra. This dataset was randomly separated into three parts: training set (80%), validation set (10%), and testing set (10%). Here, the MSE loss function and Adam optimizer were also used at the training step to obtain the optimal model, while the coefficient of determination (R^2) was selected to assess the predictive reliability of concentrations.

As a result, MSE reduced to a lower level after 200 epochs, and R^2 increased to 0.999 at the same time (Figure S8, outer). Similar results were acquired at the valid step (Figure S8, inner), and the R^2 also rose to 0.999 after 200 epochs. Also, the MSE and R^2 have been stable on the validation set after the same epochs. Therefore, the quantitation analytical model of the CNN was saved after 200 iterations on the training set. Furthermore, the CNN also has a strong generalization ability because R^2 of this model on the test set is 0.999, which had never been seen by the CNN.

Afterward, this trained model was used to analyze the concentrations of MVD in mixtures using extractive spectra. Calibration curves were first constructed to compare quantification accuracy for extractive spectra using the SENN. The concentrations range from 0.01 to 1.00 μM , and the calibration curves show high prediction coefficients of 0.999 for MVD (shown in Figure 5). In addition, several extractive pure spectra with different concentrations, which were extracted from varying mixture solutions, were passed into the quantitative model. It was more precise to predict the concentrations for both pesticides, and quantification accuracies range from 99 to 100% (Table 1). Notably, the difference between real and predicted pesticide concentrations in these samples which were selected above was 0–0.01 μM . On the other hand, the relative standard deviation (RSD) was lower than 8.8% for MVD. The CNN model also was suitable for predicting the concentrations of DDM in mixtures using

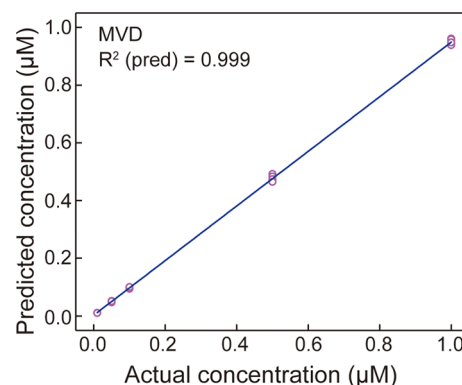


Figure 5. Calibration curve obtained using the CNN for MVD.

Table 1. Predictive Concentrations for MVD^a

$C_r/\mu\text{M}$	$C_p/\mu\text{M}$	RD/%	RSD/%
0.01	0.01	0.0	1.4
0.10	0.09	-1.0	8.8
1.00	0.99	-1.0	5.5

^aNote: C_r , real concentration; C_p , predicted concentration; RD, relative deviation; RSD, relative standard deviation.

extractive spectra with high prediction coefficients of 0.999 and an RSD of lower than 6.5% (Figure S9 and Table S1), which means that the CNN model has excellent quantitative performance.

CONCLUSIONS

In conclusion, a SENN model is proposed to extract pure spectra from mixture SERS spectra. Benefiting from functional modular design of the SENN and the narrow SERS bands suitable for multiplex detection, the SENN model can accurately extract the pure spectra from mixed SERS spectra of demonstration samples containing DDM, MVD, and TMTD with different concentrations. This demonstrates that the SENN model will be useful for expanding the analysis method of complicated samples from the qualitative aspect. Furthermore, extractive pure spectra can be used to precisely predict the concentration for per constituent using the CNN model, showing that the extractive spectra included full concentration information for each component in mixed solutions. Hence, qualitative and quantitative analysis for large-scale SERS spectra of mixture samples can be achieved by the SENN model with high performance, providing great potential as an intelligent tool in multicomponent analysis in complex environments, such as milk, blood, and so forth, by using the SERS technique.

ASSOCIATED CONTENT

Supporting Information

The Supporting Information is available free of charge at <https://pubs.acs.org/doi/10.1021/acs.jpca.1c10681>.

Au NPs' preparation; typical TEM image of Au NPs; UV–Vis spectrum of Au NPs; optimization of conditions of SERS detection; selection of the measurement concentration for constructing the dataset; violin plot of DDM, MVD, and TMTD; spectra of DDM, MVD, and TMTD and different ternary mixtures; extractive results for 24 different mixture spectra using the SENN; extractive results for mixture spectra

involving varying concentrations of DDM, MVD, and TMTD using SIMPLISMA; quantification analysis method; architecture of the one-dimension convolutional NN; training step (outer) and valid step (inner) results for the 1D-CNN model; calibration curve obtained using the CNN for DDM; and predictive concentrations for DDM ([PDF](#))

■ AUTHOR INFORMATION

Corresponding Authors

Hua-Ying Chen — Key Laboratory for Advanced Materials, Shanghai Key Laboratory of Functional Materials Chemistry, Frontiers Science Center for Materiobiology & Dynamic Chemistry, School of Chemistry & Molecular Engineering, East China University of Science and Technology, Shanghai 200237, P. R. China; Email: chenhuaying@mail.ecust.edu.cn

Da-Wei Li — Key Laboratory for Advanced Materials, Shanghai Key Laboratory of Functional Materials Chemistry, Frontiers Science Center for Materiobiology & Dynamic Chemistry, School of Chemistry & Molecular Engineering, East China University of Science and Technology, Shanghai 200237, P. R. China; orcid.org/0000-0002-9257-4452; Email: daweili@ecust.edu.cn

Authors

Jie Zhang — Key Laboratory for Advanced Materials, Shanghai Key Laboratory of Functional Materials Chemistry, Frontiers Science Center for Materiobiology & Dynamic Chemistry, School of Chemistry & Molecular Engineering, East China University of Science and Technology, Shanghai 200237, P. R. China

Pei-Lin Xin — Key Laboratory for Advanced Materials, Shanghai Key Laboratory of Functional Materials Chemistry, Frontiers Science Center for Materiobiology & Dynamic Chemistry, School of Chemistry & Molecular Engineering, East China University of Science and Technology, Shanghai 200237, P. R. China

Xiao-Yuan Wang — Key Laboratory for Advanced Materials, Shanghai Key Laboratory of Functional Materials Chemistry, Frontiers Science Center for Materiobiology & Dynamic Chemistry, School of Chemistry & Molecular Engineering, East China University of Science and Technology, Shanghai 200237, P. R. China; orcid.org/0000-0003-1646-9199

Complete contact information is available at:

<https://pubs.acs.org/10.1021/acs.jpca.1c10681>

Author Contributions

†J.Z. and P.-L.X. contributed equally.

Notes

The authors declare no competing financial interest.
Data and software availability: The dataset and SENN model architecture are available on Gitee (<https://gitee.com/JeillZhang/senn>) on the master branch. All the computing procedures are implemented by the Python programming language, where the SENN model is constructed by using PyTorch (version: 1.7.1). The other basic libraries used in preprocessing and postprocessing procedures are listed on the site mentioned above.

■ ACKNOWLEDGMENTS

The authors appreciate financial support from the National Natural Science Foundation of China (21788102, 21777041, 21974046, 22176058, and 21977031), the Science and Technology Commission of Shanghai Municipality (19391901700, 19520744000, and 19ZR1472300), and the Fundamental Research Funds for the Central Universities.

■ REFERENCES

- (1) Tzeng, Y.; Lin, B.-Y. Silver Sers Adenine Sensors with a Very Low Detection Limit. *Biosensors* **2020**, *10*, 53.
- (2) Camden, J. P.; Dieringer, J. A.; Zhao, J.; Van Duyne, R. P. Controlled Plasmonic Nanostructures for Surface-Enhanced Spectroscopy and Sensing. *Acc. Chem. Res.* **2008**, *41*, 1653–1661.
- (3) Graniel, O.; Iatsunskyi, I.; Coy, E.; Humbert, C.; Barbillon, G.; Michel, T.; Maurin, D.; Balleme, S.; Miele, P.; Bechelany, M. Au-Covered Hollow Urchin-Like Zno Nanostructures for Surface-Enhanced Raman Scattering Sensing. *J. Mater. Chem. C* **2019**, *7*, 15066–15073.
- (4) Driskell, J. D.; Kwarta, K. M.; Lipert, R. J.; Porter, M. D.; Neill, J. D.; Ridpath, J. F. Low-Level Detection of Viral Pathogens by a Surface-Enhanced Raman Scattering Based Immunoassay. *Anal. Chem.* **2005**, *77*, 6147–6154.
- (5) Stiles, P. L.; Dieringer, J. A.; Shah, N. C.; Van Duyne, R. P. Surface-Enhanced Raman Spectroscopy. *Annu. Rev. Anal. Chem.* **2008**, *1*, 601–626.
- (6) Sharma, B.; Fernanda Cardinal, M.; Kleinman, S. L.; Greeneltch, N. G.; Frontiera, R. R.; Blaber, M. G.; Schatz, G. C.; Van Duyne, R. P. High-Performance Sers Substrates: Advances and Challenges. *MRS Bull.* **2013**, *38*, 615–624.
- (7) Lu, W.; Chen, X.; Wang, L.; Li, H.; Fu, Y. V. Combination of an Artificial Intelligence Approach and Laser Tweezers Raman Spectroscopy for Microbial Identification. *Anal. Chem.* **2020**, *92*, 6288–6296.
- (8) Li, J. F.; Huang, Y. F.; Ding, Y.; Yang, Z. L.; Li, S. B.; Zhou, X. S.; Fan, F. R.; Zhang, W.; Zhou, Z. Y.; Wu, D. Y.; Ren, B.; Wang, Z. L.; Tian, Z. Q. Shell-Isolated Nanoparticle-Enhanced Raman Spectroscopy. *Nature* **2010**, *464*, 392–395.
- (9) Berger, A. G.; Restaino, S. M.; White, I. M. Vertical-Flow Paper Sers System for Therapeutic Drug Monitoring of Flucytosine in Serum. *Anal. Chim. Acta* **2017**, *949*, 59–66.
- (10) Wu, Y.; He, Y.; Yang, X.; Yuan, R.; Chai, Y. A Novel Recyclable Surface-Enhanced Raman Spectroscopy Platform with Duplex-Specific Nuclease Signal Amplification for Ultrasensitive Analysis of Microna 15S. *Sens. Actuators, B* **2018**, *275*, 260–266.
- (11) Lin, Z.; He, L. Recent Advance in Sers Techniques for Food Safety and Quality Analysis: A Brief Review. *Curr. Opin. Food Sci.* **2019**, *28*, 82–87.
- (12) Luo, X.; Liu, W.; Chen, C.; Jiang, G.; Hu, X.; Zhang, H.; Zhong, M. Femtosecond Laser Micro-Nano Structured Ag Sers Substrates with Unique Sensitivity, Uniformity and Stability for Food Safety Evaluation. *Opt. Laser. Technol.* **2021**, *139*, 106969.
- (13) Panikar, S. S.; Ramírez-García, G.; Sidhik, S.; Lopez-Luke, T.; Rodriguez-Gonzalez, C.; Ciapara, I. H.; Castillo, P. S.; Camacho-Villegas, T.; De la Rosa, E. Ultrasensitive Sers Substrate for Label-Free Therapeutic-Drug Monitoring of Paclitaxel and Cyclophosphamide in Blood Serum. *Anal. Chem.* **2018**, *91*, 2100–2111.
- (14) Fan, X.; Ming, W.; Zeng, H.; Zhang, Z.; Lu, H. Deep Learning-Based Component Identification for the Raman Spectra of Mixtures. *Analyst* **2019**, *144*, 1789–1798.
- (15) Li, Y.-T.; Qu, L.-L.; Li, D.-W.; Song, Q.-X.; Fathi, F.; Long, Y.-T. Rapid and Sensitive In-Situ Detection of Polar Antibiotics in Water Using a Disposable Ag–Graphene Sensor Based on Electrophoretic Preconcentration and Surface-Enhanced Raman Spectroscopy. *Biosens. Bioelectron.* **2013**, *43*, 94–100.
- (16) Yaseen, T.; Pu, H.; Sun, D.-W. Fabrication of Silver-Coated Gold Nanoparticles to Simultaneously Detect Multi-Class Insecticide Residues in Peach with Sers Technique. *Talanta* **2019**, *196*, 537–545.

- (17) Wang, P.; Wu, L.; Lu, Z.; Li, Q.; Yin, W.; Ding, F.; Han, H. Gecko-Inspired Nanotentacle Surface-Enhanced Raman Spectroscopy Substrate for Sampling and Reliable Detection of Pesticide Residues in Fruits and Vegetables. *Anal. Chem.* **2017**, *89*, 2424–2431.
- (18) Leong, Y. X.; Lee, Y. H.; Koh, C. S. L.; Phan-Quang, G. C.; Han, X.; Phang, I. Y.; Ling, X. Y. Surface-Enhanced Raman Scattering (Sers) Taster: A Machine-Learning-Driven Multireceptor Platform for Multiplex Profiling of Wine Flavors. *Nano Lett.* **2021**, *21*, 2642–2649.
- (19) Windig, W.; Guilment, J. Interactive Self-Modeling Mixture Analysis. *Anal. Chem.* **1991**, *63*, 1425–1432.
- (20) Zhu, Z.-L.; Cheng, W.-Z.; Zhao, Y. Iterative Target Transformation Factor Analysis for the Resolution of Kinetic–Spectral Data with an Unknown Kinetic Model. *Chemometr. Intell. Lab. Syst.* **2002**, *64*, 157–167.
- (21) Ma, Y.; Huang, P.; Hou, D.; Cai, J.; Wang, Q.; Zhang, G. The Spectral Resolution of Unknown Mixture Based on Thz Spectroscopy with Self-Modeling Technique. *Chemometr. Intell. Lab. Syst.* **2016**, *150*, 65–73.
- (22) Ezziane, Z. Applications of Artificial Intelligence in Bioinformatics: A Review. *Expert Syst. Appl.* **2006**, *30*, 2–10.
- (23) Ayres, L. B.; Gomez, F. J. V.; Linton, J. R.; Silva, M. F.; Garcia, C. D. Taking the Leap between Analytical Chemistry and Artificial Intelligence: A Tutorial Review. *Anal. Chim. Acta* **2021**, *1161*, 338403.
- (24) Guo, Z.; Wang, M.; Barimah, A. O.; Chen, Q.; Li, H.; Shi, J.; El-Seedi, H. R.; Zou, X. Label-Free Surface Enhanced Raman Scattering Spectroscopy for Discrimination and Detection of Dominant Apple Spoilage Fungus. *Int. J. Food Microbiol.* **2021**, *338*, 108990.
- (25) Zhu, J.; Sharma, A. S.; Xu, J.; Xu, Y.; Jiao, T.; Ouyang, Q.; Li, H.; Chen, Q. Rapid on-Site Identification of Pesticide Residues in Tea by One-Dimensional Convolutional Neural Network Coupled with Surface-Enhanced Raman Scattering. *Spectrochim. Acta Mol. Biomol. Spectrosc.* **2021**, *246*, 118994.
- (26) Shi, H.; Wang, H.; Meng, X.; Chen, R.; Zhang, Y.; Su, Y.; He, Y. Setting up a Surface-Enhanced Raman Scattering Database for Artificial-Intelligence-Based Label-Free Discrimination of Tumor Suppressor Genes. *Anal. Chem.* **2018**, *90*, 14216–14221.
- (27) Thrift, W. J.; Ragan, R. Quantification of Analyte Concentration in the Single Molecule Regime Using Convolutional Neural Networks. *Anal. Chem.* **2019**, *91*, 13337–13342.
- (28) Zhao, F.; Wang, W.; Zhong, H.; Yang, F.; Fu, W.; Ling, Y.; Zhang, Z. Robust Quantitative Sers Analysis with Relative Raman Scattering Intensities. *Talanta* **2021**, *221*, 121465.
- (29) Erzina, M.; Trelin, A.; Guselnikova, O.; Dvorankova, B.; Strnadova, K.; Perminova, A.; Ulbrich, P.; Mares, D.; Jerabek, V.; Elashnikov, R.; Svorcik, V.; Lyutakov, O. Precise Cancer Detection Via the Combination of Functionalized Sers Surfaces and Convolutional Neural Network with Independent Inputs. *Sens. Actuators, B* **2020**, *308*, 127660.
- (30) Russo, D. P.; Yan, X.; Shende, S.; Huang, H.; Yan, B.; Zhu, H. Virtual Molecular Projections and Convolutional Neural Networks for the End-to-End Modeling of Nanoparticle Activities and Properties. *Anal. Chem.* **2020**, *92*, 13971–13979.
- (31) Llorent-Martínez, E. J.; Ortega-Barrales, P.; Fernández-de Córdoba, M. L.; Ruiz-Medina, A. Trends in Low-Based Analytical Methods Applied to Pesticide Detection: A Review. *Anal. Chim. Acta* **2011**, *684*, 30–39.
- (32) Buffa, A.; Mandler, D. Adsorption and Detection of Organic Pollutants by Fixed Bed Carbon Nanotube Electrochemical Membrane. *Chem. Eng. J.* **2019**, *359*, 130–137.
- (33) Stavra, E.; Petrou, P. S.; Koukouvinos, G.; Kiritsis, C.; Pirmettis, I.; Papadopoulos, M.; Goustouridis, D.; Economou, A.; Misiakos, K.; Raptis, I.; Kakabakos, S. E. Simultaneous Determination of Paraquat and Atrazine in Water Samples with a White Light Reflectance Spectroscopy Biosensor. *J. Hazard. Mater.* **2018**, *359*, 67–75.
- (34) Acharya, U. R.; Oh, S. L.; Hagiwara, Y.; Tan, J. H.; Adeli, H.; Subha, D. P. Automated Eeg-Based Screening of Depression Using Deep Convolutional Neural Network. *Comput. Methods Progr. Biomed.* **2018**, *161*, 103–113.
- (35) Li, Y.; Wang, N.; Shi, J.; Hou, X.; Liu, J. Adaptive Batch Normalization for Practical Domain Adaptation. *Pattern Recogn.* **2018**, *80*, 109–117.
- (36) Jolliffe, I. T.; Cadima, J. Principal Component Analysis: A Review and Recent Developments. *Philos. Trans. R. Soc., A* **2016**, *374*, 20150202.

□ Recommended by ACS

Differentiation of NaCl, NaOH, and β-Phenylethylamine Using Ultraviolet Spectroscopy and Improved Adaptive Artificial Bee Colony Combined with BP-ANN Algorithm

Angxin Tong, Qiang Zhang, et al.

MARCH 20, 2023

ACS OMEGA

READ ▶

Potential Regulation for Surface-Enhanced Raman Scattering Detection and Identification of Carotenoids

Haifeng Zhou and Janina Kneipp

FEBRUARY 02, 2023

ANALYTICAL CHEMISTRY

READ ▶

Deep Learning-Based Multicapturer SERS Platform on Plasmonic Nanocube Metasurfaces for Multiplex Detection of Organophosphorus Pesticides in Environmental Water

Ruili Li, Xiaoqing Chen, et al.

NOVEMBER 08, 2022

ANALYTICAL CHEMISTRY

READ ▶

Stretchable and Flexible Micro-Nano Substrates for SERS Detection of Organic Dyes

Yuanhang Tan, Changguo Xue, et al.

APRIL 11, 2023

ACS OMEGA

READ ▶

Get More Suggestions >